First-principles study of the structure, electronic, and optical properties of orthorhombic $BiInO_3$

Chenliang Li and Hai WangBiao WangRui Wang

Citation: Appl. Phys. Lett. **91**, 071902 (2007); doi: 10.1063/1.2770761
View online: http://dx.doi.org/10.1063/1.2770761
View Table of Contents: http://aip.scitation.org/toc/apl/91/7
Published by the American Institute of Physics

First-principles study of the structure, electronic, and optical properties of orthorhombic $BiInO_3$

Chenliang Li and Hai Wang
School of Astronautics, Harbin Institute of Technology, Harbin, Heilongjiang 150001, China

Biao Wang[a)]
State Key Laboratory of Optoelectronic Materials and Technologies, Sun Yat-Sen University, Guangzhou 510275, China; Institute of Optoelectronic and Functional Composite Materials, Sun Yat-Sen University, Guangzhou 510275, China; and School of Physics and Engineering, Sun Yat-Sen University, Guangzhou 510275, China

Rui Wang
Department of Applied Chemistry, Harbin Institute of Technology, Harbin, Heilongjiang 150001, China

(Received 29 May 2007; accepted 20 July 2007; published online 13 August 2007)

The structural, electronic, and optical properties of orthorhombic $BiInO_3$ were investigated in the framework of the density functional theory. The calculated structural parameters are in agreement with the experimental data. The band structure, density of states, and Mulliken charge population are obtained, which indicates that $BiInO_3$ has an indirect band gap of 2.08 eV. Furthermore, its optical properties are also calculated and analyzed in details. It is shown that $BiInO_3$ is a promising dielectric material. © *2007 American Institute of Physics*. [DOI: 10.1063/1.2770761]

Recently, $BiMO_3$ (M=Mn, Fe, Al, Ga, Sc, In) have received tremendous attention as multiferroics.[1–3] It is also used to fabricate the $BiMO_3$–$PbTiO_3$ solid solutions to improve ferroelectric properties of $PbTiO_3$ and reduce the amount of lead.[4–9] Among these compounds, multiferroic $BiMnO_3$ and $BiFeO_3$ have been extensively investigated.[10–14] $BiScO_3$ has also been studied using both experimental and theoretical methods.[8,9,15] It was suggested that $BiScO_3$ could substitute for $PbZrO_3$ in $Pb(Zr,Ti)O_3$, and Baetting *et al.*[16] theoretically predicted the large ferroelectric polarization and piezoelectricity in the hypothetical perovskite-structure oxides $BiAlO_3$ and $BiGaO_3$. Later on, Belik *et al.*[17] prepared $BiAlO_3$ and $BiGaO_3$ using high-pressure high-temperature techniques. $BiInO_3$, as a noncentrosymmetric compound, was synthesized under high pressure by Belik *et al.*[18] in 2006. Noncentrosymmetric compounds have been attractive because of their important properties, such as piezoelectricity, ferroelectricity, and pyroelectricity, as well as second-order nonlinear optical behaviors.[19] At present, there are no reports about electronic and optical properties of orthorhombic $BiInO_3$. In this work, we present a series of first-principles density function calculations on the structural, electronic, and optical properties of $BiInO_3$ material.

The calculations were performed using the plane-wave pseudopotential method based on the density functional theory (DFT) with the generalized gradient approximation (GGA) in the scheme of Perdew–Burke–Ernzerhof.[20] The ion-electron interaction was modeled by ultrasoft Vanderbilt-type pseudopotentials.[21] Mulliken charges were calculated according to the formalism described by Segall *et al.*[22] A plane-wave cutoff energy of 400 eV was employed throughout the calculation. For the sampling of the Brillouin zone, the electronic structures and optical properties used $8\times8\times6$ and $10\times10\times12$ k-point grids generated according to the Monkhorst-Pack scheme,[23] respectively.

The optical properties of $BiInO_3$ is determined by the frequency-dependent dielectric function $\varepsilon(\omega)=\varepsilon_1(\omega)+i\varepsilon_2(\omega)$ that is mainly connected with the electronic structures. The imaginary part $\varepsilon_2(\omega)$ of the dielectric function $\varepsilon(\omega)$ is calculated from the momentum matrix elements between the occupied and unoccupied electronic states and given by

$$\varepsilon_2=\frac{2e^2\pi}{\Omega\varepsilon_0}\sum_{k,v,c}|\langle\psi_k^c|\hat{u}\cdot r|\psi_k^v\rangle|^2\delta(E_k^c-E_k^c-E),$$

where ω is the light frequency, e is the electronic charge, and ψ_k^c and ψ_k^v are the conduction and valence band wave functions at k, respectively. The real part $\varepsilon_1(\omega)$ is derived from the imaginary part $\varepsilon_2(\omega)$ by the Kramers-Kronig transformation. All other optical constants, such as the absorption spectrum, refractive index, and reflectivity are derived from $\varepsilon_1(\omega)$ and $\varepsilon_2(\omega)$.[24]

$BiInO_3$ belongs to $GdFeO_3$-type perovskite structure with a space group $Pna2_1$. We used the x-ray diffraction data[18] as a starting point for geometry optimization. The lattice parameters and bulk modulus were calculated and fitted to third order Birch-Murnaghan equation of states.[25] The results are summarized in Table I. Our calculated lattice parameters are in agreement with the experimental data.

The energy band structure and densities of states (DOSs) of $BiInO_3$ are shown in Figs. 1 and 2, respectively. The energy band structure is calculated along the high-symmetry directions in the Brillouin zone.

TABLE I. Calculated and experimental lattice parameters, bulk modulus (B_0), and its pressure derivative (B_0') of orthorhombic $BiInO_3$.

		a (Å)	b (Å)	c (Å)	V (Å^3)	B_0 (GPa)	$B_0^{'}$
	Cal.[a]	5.993	5.777	8.255	285.80	94	8.27
$BiInO_3$	Expt.[b]	5.955	5.602	8.386	279.74		

[a]This work.
[b]Reference 22.

[a)]Author to whom correspondence should be addressed; electronic mail: lichenliang1980@yahoo.com.cn

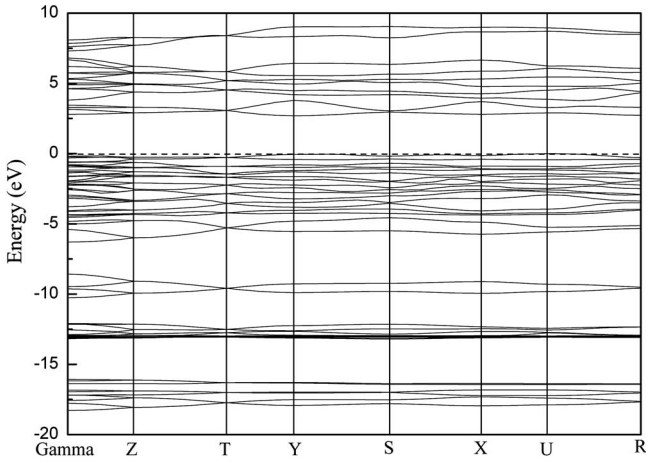

FIG. 1. Energy band structure of orthorhombic $BiInO_3$.

The top of the valence band (VB) and the bottom of the conduction band (CB) are composed of O 2*p* states and Bi 6*p* states, respectively. In contrast, the band gap of $PbTiO_3$ ($PbZrO_3$) is determined by O 2*p* states and Ti 3*d* (Zr 4*d*) states rather than those associated with Pb–O. $BiInO_3$ presented an indirect band gap of 2.08 eV connecting the *U* (VB) and *Y* (CB) points. The band gaps predicted by the DFT are smaller than experimental data, which means that our results underestimate the real band gaps of $BiInO_3$. In our calculation, the scissor operators on both the electronic structure and the optical properties were not considered. The energy bands between −20 and −15 eV mainly consist of O 2*s* states. The energy bands at about −13 eV consist of In 4*d* states showed a sharp peak due to its strong localization character. The Bi 6*s* states were located at about −10 eV. By analyzing the partial density of states (PDOS), it was found that the O 2*p* states have some admixture with the Bi and In *sp* states. Thus, $BiInO_3$ appears to have some covalent features. Moreover, in the region of the valence band, the width of the PDOS of Bi was clearly narrower than that of In and O. The number of peaks was also less than those for In. This indicates that the hybridization of In–O is stronger than that for Bi–O. Above 7 and up to 10 eV, the energy bands derived from the In 5*p* and 5*s* states, which force Bi 6*p* states to move towards the Fermi level. Based on the foregoing results, it is clear that the electronic properties of $BiInO_3$ are affected by the In ion through their influence on the Bi–O bonding.

We also performed the Mulliken charge population for $BiInO_3$ to understand bonding behavior. The Mulliken population results are given in Table II. The charge transfer from Bi and In to O are about 1.61*e*, 1.12*e*, respectively. Therefore, we concluded that the bonding behavior of $BiInO_3$ is a combination of covalent and ionic natures. Moreover, the In–O bond possessed a stronger covalent bonding strength than the Bi–O bond. The results are consistent with our DOS calculation.

The calculated dielectric function of $BiInO_3$ is shown in Fig. 3. We only considered the case of the incident radiation with the linear polarization along the [001] direction. For the imaginary part $\varepsilon_2(\omega)$ of the dielectric function, peaks A (4.19 eV), B (5.89 eV), and C (8.89 eV) correspond to the transition from O 2*p* VB to Bi 6*p* CB, and peak D (14.37 eV) corresponds to the transition from O 2*p* VB to In 5*s* CB. Peaks E (24.79 eV) and F (27.49 eV) are ascribed to

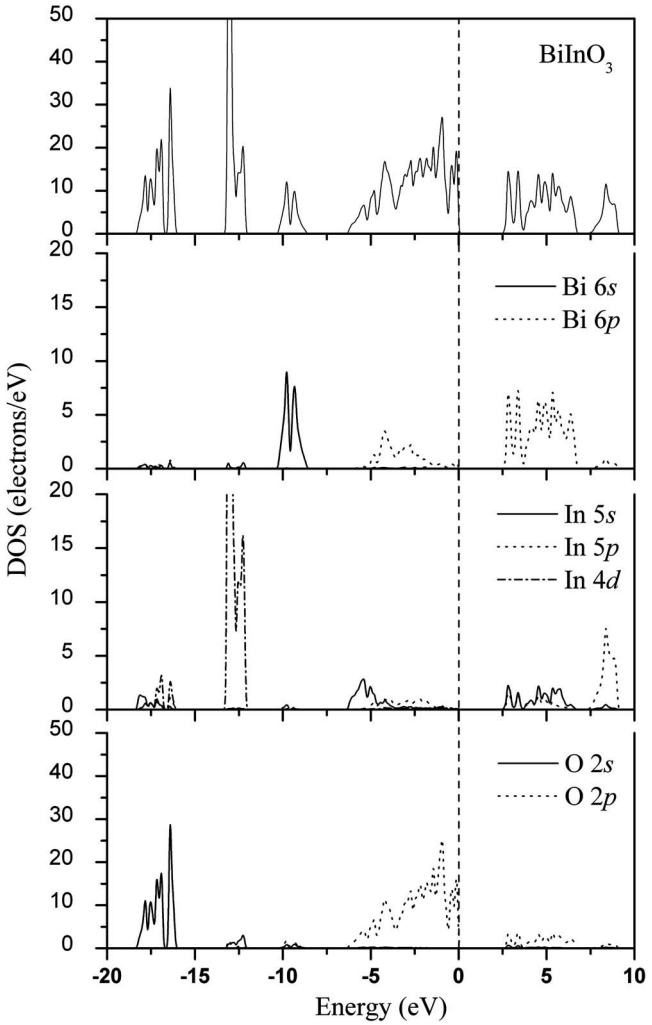

FIG. 2. Total and partial DOS of orthorhombic $BiInO_3$.

the transition of inner electron excitation from O 2*s* and Bi 6*s* levels to CB. The calculated static dielectric constant $\varepsilon_1(0)$ was found to be 6.75, which is larger than those of $BaTiO_3$ (5.12), $SrTiO_3$ (4.98), and $PbZrO_3$ (5.34). It is reasonable to expect that $BiInO_3$ is a promising dielectric material.

The calculated results on the absorption spectrum, refractive index, extinction coefficient, reflectivity, and energy-loss spectrum are also shown in Figs. 4(a)–4(e). In our calculation, we used Gaussian smearing which is 0.5 eV. The absorption spectrum started at 2.12 eV and decreased rapidly in the low-energy region. In the range from 0 to 2.12 eV, the reflectivity was lower than 25%, which indicates that $BiInO_3$ material is transmitting for frequencies less than 2.12 eV. The energy-loss spectrum describes the energy loss of a fast electron traversing in the material and is usually large at the

TABLE II. Mulliken charge population of orthorhombic $BiInO_3$.

Species	*s*	*p*	*d*	Total	Charge (*e*)
Bi	1.69	1.70	0.00	3.39	1.61
In	0.91	0.98	9.99	11.88	1.12
O(1)	1.91	4.99	0.00	6.89	−0.89
O(2)	1.89	5.04	0.00	6.93	−0.93
O(3)	1.90	5.01	0.00	6.91	−0.91

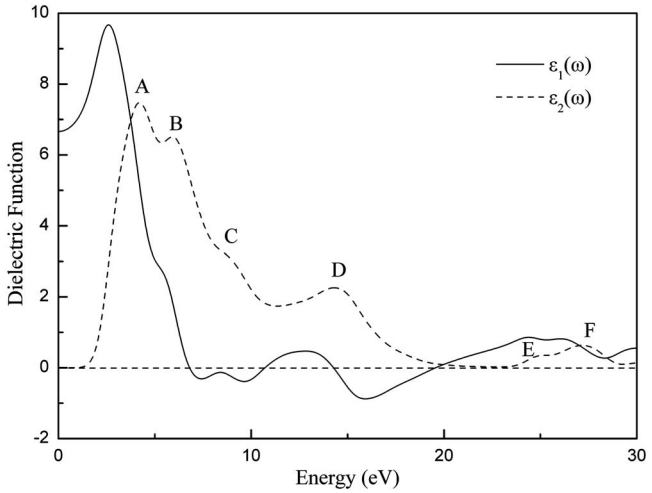

FIG. 3. Imaginary part $\varepsilon_2(\omega)$ and real part $\varepsilon_1(\omega)$ of the dielectric function $\varepsilon(\omega)$ of orthorhombic $BiInO_3$.

plasma energy.[26] The energy-loss spectrum of $BiInO_3$ presented four prominent peaks which are consistent to the roots of $\varepsilon_1(\omega)$. Moreover, the sharp structure at about 20 eV corresponds to a rapid reduction of the reflectance. This process is associated with the transitions from the filled O 2*s* and Bi 6*s* bands to empty CB. The calculated static refractive index was found to be 2.58.

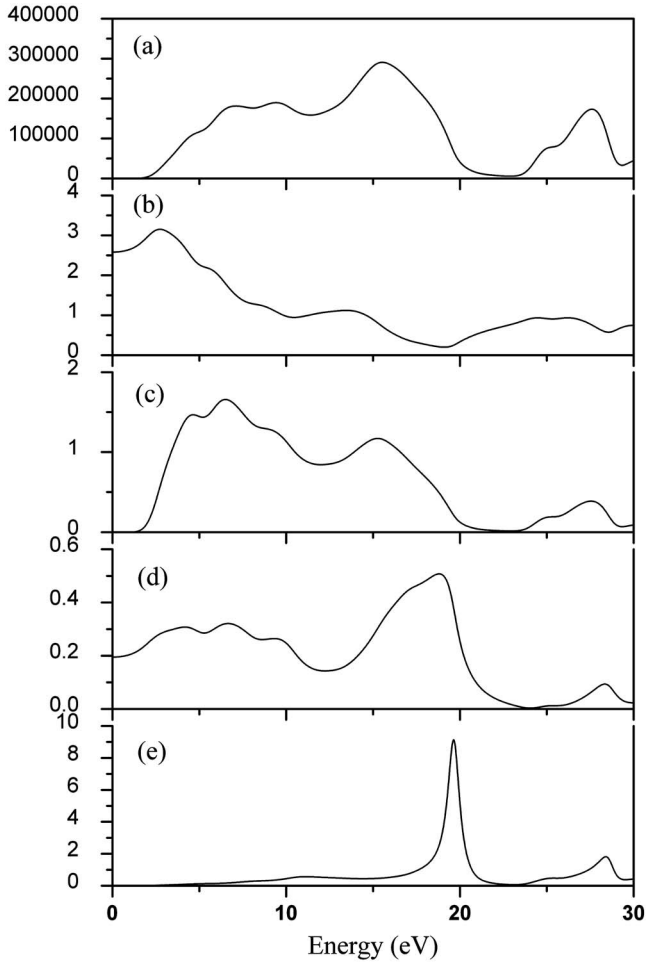

FIG. 4. Optical constants of orthorhombic $BiInO_3$. (a) Absorption spectrum, (b) refractive index, (c) extinction coefficient, (d) reflectivity, and (e) energy-loss spectrum.

In summary, we calculated the structural parameters, electronic structures, and optical properties for orthorhombic $BiInO_3$ by means of the DFT within the GGA. Our structural parameters are in agreement with the experimental data. The electronic structures of $BiInO_3$ revealed that the top of the valence band and the bottom of the conduction band are decided by O 2*p* and Bi 6*p* states, respectively, and that $BiInO_3$ presented an indirect band gap of 2.08 eV. Furthermore, the In–O bond possesses a stronger covalent bonding strength than the Bi–O bond. Finally, the dielectric function, absorption spectrum, refractive index, extinction coefficient, reflectivity, and energy-loss spectrum were obtained and discussed in detail. It is shown that $BiInO_3$ is a promising dielectric material.

This work was supported by the National Natural Science Foundation of China (Grant Nos. 10572155, 10172030, and 50232030) and The Science Foundation of Guangdong Province Grant No. (2005A10602002).

[1] M. Fiebig, J. Phys. D **38**, R123 (2005).
[2] W. Prellier, M. P. Singh, and P. Murugavel, J. Phys. Condens. Matter **17**, R803 (2005).
[3] N. A. Hill, J. Phys. Chem. B **104**, 6694 (2000).
[4] S. J. Zhang, C. A. Randall, and T. R. Shrout, Appl. Phys. Lett. **83**, 3150 (2003).
[5] T. Yoshimura and S. Trolier-McKinstry, Appl. Phys. Lett. **81**, 2065 (2002).
[6] J. R. Cheng, W. Y. Zhu, N. Li, and L. E. Cross, Mater. Lett. **57**, 2090 (2003).
[7] J. Cheng, R. Eitel, N. Li, and L. E. Cross, J. Appl. Phys. **94**, 605 (2003).
[8] S. V. Halilov, M. Fornari, and D. J. Singh, Phys. Rev. B **69**, 174107 (2004).
[9] J. Iniguez, D. Vanderbilt, and L. Bellaiche, Phys. Rev. B **67**, 224107 (2003).
[10] T. Atou, H. Chiba, K. Ohoyama, Y. Yamaguchi, and Y. Syono, J. Solid State Chem. **145**, 639 (1999).
[11] E. Montanari, L. Righi, G. Calestani, A. Migliori, E. Gilioli, and F. Bolzoni, Chem. Mater. **17**, 1765 (2005).
[12] J. B. Neaton, C. Ederer, U. V. Waghmare, N. A. Spaldin, and K. M. Rabe, Phys. Rev. B **71**, 014113 (2005).
[13] F. Kubel and H. Schmid, Acta Crystallogr., Sect. B: Struct. Sci. **46**, 698 (1990).
[14] J. Wang, J. B. Neaton, H. Zheng, V. Nagarajan, S. B. Ogale, B. Liu, D. Viehland, V. Vaithyanathan, D. G. Schlom, U. V. Waghmare, N. A. Spaldin, K. M. Rabe, M. Wuttig, and R. Ramesh, Science **299**, 1719 (2003).
[15] A. A. Belik, S. Likubo, K. Kodama, N. Igawa, S. Shamoto, M. Maie, T. Nagai, Y. Matsui, S. Yu. Stefanovich, B. I. Lazorvak, and E. Takayama-Muromachi, J. Am. Chem. Soc. **128**, 706 (2006).
[16] P. Baetting, C. F. Schelle, R. LeSar, U. V. Waghmare, and N. A. Spaldin, Chem. Mater. **17**, 1376 (2005).
[17] A. A. Belik, T. Wuernisha, T. Kamiyama, K. Mori, M. Maie, T. Nagai, Y. Matsui, and E. Takayama-Muromachi, Chem. Mater. **18**, 133 (2006).
[18] A. A. Belik, S. Y. Stefanovich, B. I. Lazoryak, and E. Takayama-Muromachi, Chem. Mater. **18**, 1964 (2006).
[19] P. S. Halasyamani and K. R. Poeppelmeier, Chem. Mater. **10**, 2753 (1998).
[20] J. P. Perdew, K. Burke, and M. Ernzerhof, Phys. Rev. Lett. **77**, 3865 (1996).
[21] D. Vanderbilt, Phys. Rev. B **41**, 7892 (1990).
[22] M. D. Segall, C. J. Pickard, R. Shah, and M. C. Payne, Mol. Phys. **89**, 571 (1996).
[23] H. J. Monkhorst and J. D. Pack, Phys. Rev. B **13**, 5188 (1976).
[24] S. Saha, T. P. Sinha, and A. Mookerjee, Phys. Rev. B **62**, 8828 (2000).
[25] F. Birch, J. Geophys. Res. **83**, 1257 (1978).
[26] M. Xu, S. Y. Wang, G. Yin, J. Li, Y. X. Zheng, and L. Y. Chen, Appl. Phys. Lett. **89**, 151908 (2006).